e-ISSN:2582-7219

INTERNATIONAL JOURNAL OF MULTIDISCIPLINARY RESEARCH IN SCIENCE, ENGINEERING AND TECHNOLOGY

Volume 7, Issue 9, September 2024

INTERNATIONAL STANDARD SERIAL NUMBER INDIA

Impact Factor: 7.521

6381 907 438 6381 907 438 ijmrset@gmail.com www.ijmrset.com

© 2024 IJMRSET | Volume 7, Issue 9, September 2024| DOI: 10.15680/IJMRSET.2024.0709011

ISSN: 2582-7219 | www.ijmrset.com | Impact Factor: 7.521| ESTD Year: 2018|

International Journal of Multidisciplinary Research in Science, Engineering and Technology (IJMRSET)

(A Monthly, Peer Reviewed, Refereed, Scholarly Indexed, Open Access Journal)

Structural and Phase Study of $Co_{1-x}Zn_xFe_2O_4$ (x = 0.8) NPs with Electrical and Magnetic Analysis

Ram S. Barkule[1], Sudarshana G. Badhe[2], Santosh D. More[3]

Department of Physics, Sundarrao More Arts, Commerce and Science College, Poladpur, Raigad, India[1]

Department of Physics, R.B. Attal Arts, Science and Commerce College, Georai, Beed, India[2]

Department of Physics, Deogiri College, Chhatrapati Sambhajinagar, India[3]

ABSTRACT: This study presents the synthesis and detailed characterization of $Co_{0.2}Zn_{0.8}Fe_2O_4$ nanoparticles (NPs) utilizing a wet chemical approach. The NPs were synthesized through a gel combustion method, resulting in a single-phase cubic spinel structure as confirmed by X-ray diffraction (XRD). Fourier-transform infrared spectroscopy (FTIR) revealed characteristic metal-oxygen bond vibrations, affirming the successful incorporation of metal ions into the spinel lattice. Direct current (DC) resistivity measurements indicated a thermally activated conduction mechanism with an activation energy of 0.41 eV. Magnetic analysis using a vibrating sample magnetometer (VSM) demonstrated pronounced ferromagnetic properties with a saturation magnetization of 0.65 emu/g, coercivity of 130 Oe, and remanent magnetization of 0.32 emu/g. These findings highlight the potential of $Co_{0.2}Zn_{0.8}Fe_2O_4$ NPs for applications in semiconductor technology, nanosensors, and biomedical devices, given their favorable structural, electrical, and magnetic properties.

KEYWORDS: X-ray diffraction; SEM; DC-electric resistivity; Magnetic Property.

I. INTRODUCTION

Spinel ferrites are a remarkable class of magnetic materials known for their distinctive structural, magnetic, and electrical properties. They are described by the general formula MFe_2O_4, where M represents a divalent metal cation, which can include ions such as Fe^{2+}, Co^{2+}, Ni^{2+}, Cu^{2+}, Mg^{2+}, or Zn^{2+}. This versatility in cation choice allows spinel ferrites to be highly customizable, leading to a wide range of physical and chemical properties tailored to specific applications. The spinel ferrite structure is derived from a cubic close-packed arrangement of oxygen anions, creating a lattice that can accommodate metal cations in two types of sites: tetrahedral (A) and octahedral (B) [1, 2]. This arrangement enables spinel ferrites to exhibit unique magnetic properties, such as ferrimagnetism, where the opposing magnetic moments of the cations result in a net magnetic moment [3]. The ability to modify the type and concentration of metal cations allows for precise control over the material's magnetic behavior, electrical conductivity, and other physical characteristics [4]. Due to these tunable properties, spinel ferrites find extensive use across various technological domains. In electronics, they are employed in applications such as inductors and transformers due to their high magnetic permeability and low electrical conductivity. In catalysis, their high surface area and stability make them effective catalysts for various chemical reactions. Their magnetic properties are harnessed in magnetic storage devices, where they enable high-density data storage. In biomedical technologies, spinel ferrites are explored for applications like magnetic resonance imaging (MRI) contrast agents [5], targeted drug delivery systems [6], and hyperthermia treatment for cancer [7, 8]. The versatility of spinel ferrites, coupled with their ability to be engineered for specific applications, underscores their importance in advancing various technological fields. By leveraging the unique properties of these materials, researchers and engineers can develop innovative solutions to meet the demands of modern technology and industry. The crystal structure of spinel ferrites is primarily based on a cubic close-packed arrangement of oxygen anions, which provides a framework for the placement of metal cations. In this arrangement, there are 64 tetrahedral (A) sites and 32 octahedral (B) sites available for cation occupancy. However, due to the stoichiometry of the material, only a fraction of these sites are typically filled. In a typical spinel structure, about 8 out of 64 A sites and 16 out of 32 B sites are occupied by metal cations, leading to a distinct distribution of cations that influences the material's properties [9, 10]. A critical parameter that affects the structural and physical properties of spinel ferrites is the oxygen position parameter, denoted as u. This parameter measures the displacement of oxygen

ISSN: 2582-7219 | www.ijmrset.com | Impact Factor: 7.521| ESTD Year: 2018|

International Journal of Multidisciplinary Research in Science, Engineering and Technology (IJMRSET)

(A Monthly, Peer Reviewed, Refereed, Scholarly Indexed, Open Access Journal)

atoms from their ideal positions within the unit cell. In an ideal spinel configuration, oxygen anions are symmetrically distributed, but real crystals often exhibit slight deviations from this ideal arrangement. The oxygen parameter (u) plays a significant role in determining the distances between cations and oxygen anions, which in turn influences bond lengths and angles between metal cations at both tetrahedral (A) and octahedral (B) sites [11]. Minor changes in the oxygen position parameter can significantly alter the strength of super-exchange interactions among cations, particularly those at the B sites, which are crucial for determining magnetic properties. Variations in this parameter also impact the lattice constant and electronic structure of spinel ferrites, thereby modifying their dielectric and optical properties. Understanding and controlling the oxygen position parameter is essential for optimizing material properties for specific applications. This parameter can be adjusted through different synthesis methods, doping with alternative cations, or thermal treatments. Even small variations in the u parameter, particularly within the range of 0.25 to 0.27, can lead to significant changes in the performance of spinel ferrites.

Magnetic Properties and Their Applications

The magnetic properties of spinel ferrites are primarily influenced by the arrangement and type of cations present in their crystal lattice, specifically in the tetrahedral (A) and octahedral (B) sites. The distribution of these cations plays a crucial role in determining the ferrite's overall magnetic characteristics, such as coercivity, saturation magnetization, and magnetic ordering. **Cobalt Ferrite ($CoFe_2O_4$):** Cobalt ferrite is an example of an inverse spinel structure, where trivalent iron ions (Fe^{3+}) occupy the tetrahedral (A) sites, while the octahedral (B) sites are occupied by a mix of divalent cobalt ions (Co^{2+}) and trivalent iron ions (Fe^{3+}) [12]. This specific arrangement results in strong ferrimagnetism, characterized by high magnetic coercivity and saturation magnetization. The high coercivity of $CoFe_2O_4$ makes it highly resistant to changes in its magnetic state, which is beneficial for applications requiring stable magnetic properties. Its high saturation magnetization is indicative of its strong magnetic response to an applied magnetic field. Consequently, cobalt ferrite is extensively used in magnetic storage devices, magnetic sensors, and actuators where robust and reliable magnetic performance is essential. **Zinc Ferrite ($ZnFe_2O_4$):** Zinc ferrite, on the other hand, can exhibit different magnetic and electrical properties due to its unique cation distribution. In a typical zinc ferrite structure, divalent zinc ions (Zn^{2+}) and trivalent iron ions (Fe^{3+}) occupy the A and B sites, respectively [13]. However, when zinc ferrite is synthesized at the nanoscale through methods such as sol-gel auto-combustion, annealing conditions can significantly affect its properties. For example, increasing the annealing temperature can cause a reduction in the number of Fe^{3+} cations in the B sites, possibly due to the oxidation of Zn^{2+} to Zn^{3+} [14]. This substitution of zinc ions can profoundly alter the ferrite's magnetic and electrical behavior. Nanosized $ZnFe_2O_4$ powders, particularly those synthesized under varying thermal conditions, have been shown to exhibit changes in magnetic and electrical properties that make them suitable for diverse applications. These include photocatalysis, where their ability to generate reactive oxygen species is utilized for environmental remediation; drug delivery, where their magnetic properties aid in targeting and controlling drug release; and energy storage, where their unique properties contribute to improved performance in batteries and supercapacitors. The ability to tailor the magnetic and electrical properties of spinel ferrites through cation arrangement and synthesis conditions underscores their versatility and potential for specialized applications. By adjusting the synthesis parameters and the composition of spinel ferrites, researchers can develop materials with optimized properties for a wide range of technological and industrial uses [15].

Influence of Doping and Synthesis Methods

The ability to tailor the properties of spinel ferrites through cation substitution and controlled synthesis methods is a significant advantage of these materials. For example, in Zn-doped $CoFe_2O_4$ nanoparticles, increasing the concentration of Zn^{2+} ions from x = 0.0 to x = 0.8 results in a larger lattice parameter, due to the larger ionic radius of Zn^{2+} compared to Co^{2+} [16]. This increase in lattice parameter is accompanied by a rise in spontaneous magnetization, enhancing the material's performance in magnetic applications. Spinel ferrites can be synthesized using various methods, such as sol-gel auto-combustion, hydrothermal synthesis, and high-temperature solid-state reactions, each offering precise control over the material's composition and structural characteristics [15]. These methods enable the production of nanoparticles with specific sizes, uniformity, and purity. The versatility of spinel ferrites is further demonstrated by their broad range of applications, including photocatalysis for environmental remediation, biosensors for detecting biological molecules, catalysts for chemical reactions [17], magnetic refrigeration technologies [18], permanent magnets [19], and biomedical uses like drug delivery and hyperthermia treatment [20]. By adjusting synthesis

© 2024 IJMRSET | Volume 7, Issue 9, September 2024| DOI: 10.15680/IJMRSET.2024.0709011

ISSN: 2582-7219 | www.ijmrset.com | Impact Factor: 7.521| ESTD Year: 2018|

International Journal of Multidisciplinary Research in Science, Engineering and Technology (IJMRSET)

(A Monthly, Peer Reviewed, Refereed, Scholarly Indexed, Open Access Journal)

parameters and doping levels, researchers can fine-tune the material's properties, making spinel ferrites highly adaptable and valuable for various technological and industrial purposes.

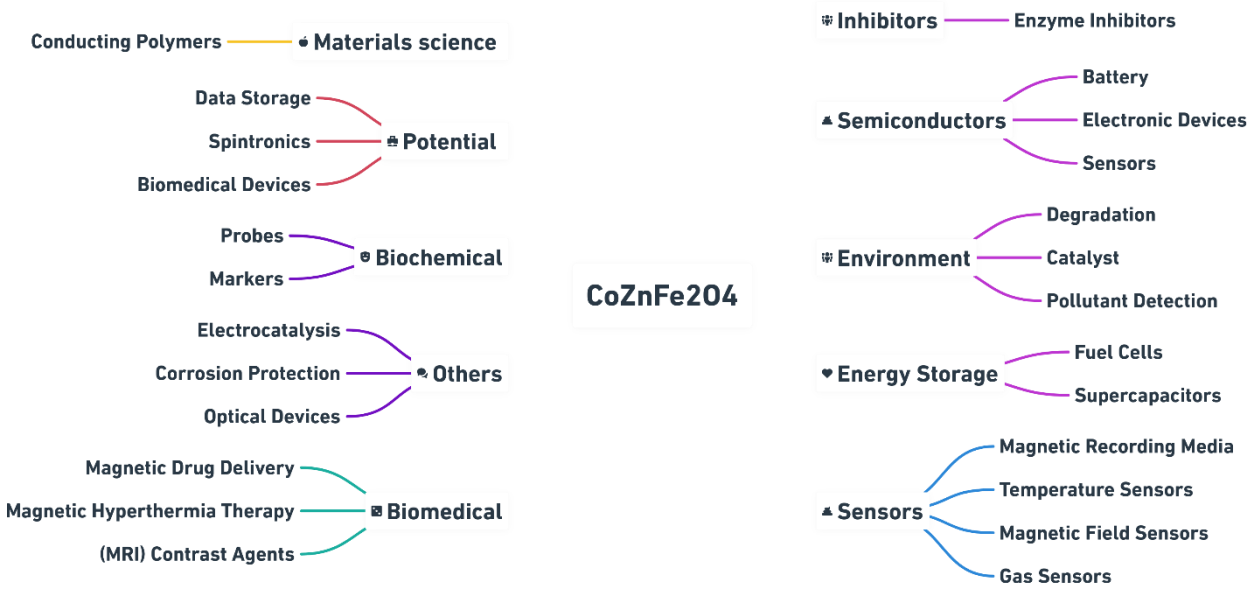

Figure 1 Various Applications of Spinel Ferrite

II. EXPERIMENTAL METHOD

Starting Materials:

The synthesis of spinel-structured $Co_{1-x}Zn_xFe_2O_4$ nanoparticles with varying compositions, specifically where x = 0.8, was conducted using high-purity starting materials that required no additional purification. The materials employed included cobalt nitrate hexahydrate ($Co(NO_3)_2 \cdot 6H_2O$), zinc nitrate tetrahydrate ($Zn(NO_3)_2 \cdot 4H_2O$), and ferric nitrate nonahydrate ($Fe(NO_3)_3 \cdot 9H_2O$), all possessing a purity level of 99.9%. Citric acid was utilized as a complexing agent during the synthesis to promote the formation of the desired spinel structure. The ratio of metal nitrates to the fuel ($C_6H_5O_7^{3-}$) was meticulously maintained at 1:3 to ensure optimal reaction conditions. This specific ratio is essential for creating a stable metal-citrate complex, which is vital for producing homogeneous and well-defined nanoparticles. Additionally, ammonia solution (NH_4OH) was used to adjust and stabilize the pH at 8 throughout the synthesis process. Controlling the pH is critical for achieving the desired properties and composition of the nanoparticles, as it affects the solubility and stability of the metal-citrate complexes. This meticulous approach enables the fine-tuning of the nanoparticles' composition and characteristics, facilitating the successful production of $Co_{0.2}Zn_{0.8}Fe_2O_4$ nanoparticles with specific attributes for various applications. By employing high-purity starting materials, optimizing the metal nitrate to citric acid ratio, and carefully regulating the pH during synthesis, researchers can effectively create spinel-structured $Co_{0.2}Zn_{0.8}Fe_2O_4$ nanoparticles with tailored compositions and properties. Such precise control is crucial for the development of advanced materials intended for specific applications, including catalysis, energy storage, and magnetic devices.

III. SYNTHESIS OF $CO_{1-X}ZN_XFE_2O_4$ (X=0.8) NANOPARTICLES

Synthesis Method:

The wet chemical synthesis method was developed to produce $Co_{1-x}Zn_xFe_2O_4$ (x=0.8) nanoparticles, valued for their unique magnetic and electrical properties, making them ideal for applications in catalysis, energy storage, and biomedical technologies. The process begins by combining high-purity cobalt and ferric nitrates in deionized water, which helps avoid impurities. The solution is stirred and homogenized to ensure even metal ion distribution [21].

© 2024 IJMRSET | Volume 7, Issue 9, September 2024| DOI: 10.15680/IJMRSET.2024.0709011

ISSN: 2582-7219 | www.ijmrset.com | Impact Factor: 7.521| ESTD Year: 2018|

International Journal of Multidisciplinary Research in Science, Engineering and Technology (IJMRSET)

(A Monthly, Peer Reviewed, Refereed, Scholarly Indexed, Open Access Journal)

Citric acid is used as a complexing agent to stabilize the metal ions, and the solution is heated to 80°C to concentrate it by evaporating excess water. Ammonia solution is added to maintain a pH of 8, essential for forming metal hydroxides. The solution transitions from a colloidal suspension to a viscous brown gel, indicating successful precursor formation. Increasing the temperature to 110°C initiates a self-propagating auto-combustion process that results in a loose powder of pre-sintered $Co_{1-x}Zn_xFe_2O_4$ (x=0.8). This method, including the sol-gel auto-combustion approach, is advantageous for its simplicity, cost-effectiveness, and ability to produce nanoparticles with controlled size and morphology. The resulting $Co_{1-x}Zn_xFe_2O_4$ (x=0.8) nanoparticles are highly suitable for various advanced applications, and ongoing research aims to optimize their synthesis for improved performance in emerging technologies [22].

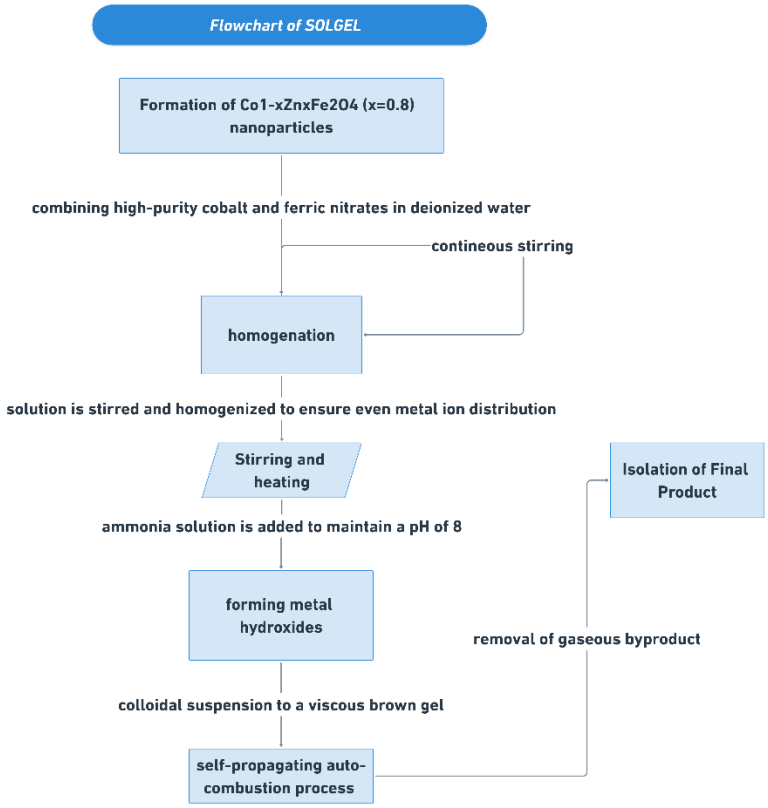

Figure 2 General Synthetic route for $Co_{1-x}Zn_xFe_2O_4$ (x=0.8) nanoparticles via solgel auto-combustion method

IV. RESULTS AND DISCUSSION

X-ray diffraction

The crystal Structural examination of $Co_{1-x}Zn_xFe_2O_4$ (x=0.8) NPs were carried out using X-ray diffraction (XRD) with a X'PertPRO MPD PANalytical system. The analysis was kept spanned a 2θ range from 20º to 80º, using the Cu-Kα radiation with a wavelength of λ = 1.5405 Å at RT. The XRD pattern, i.e. shown in **Figure 1**, indicated that the $Co_{0.2}Zn_{0.8}Fe_2O_4$ NPs exhibits a single-phase cubic spinel structure [23] (see **Figure 2**). No extra peak was detected in the XRD pattern. The X-ray diffraction pattern confirmed the presence of specific planes, including (220), (311), (400), (422), (511), (440), and (622), [24] as detailed in **Table 1**.

© 2024 IJMRSET | Volume 7, Issue 9, September 2024| DOI: 10.15680/IJMRSET.2024.0709011

ISSN: 2582-7219 | www.ijmrset.com | Impact Factor: 7.521| ESTD Year: 2018|

International Journal of Multidisciplinary Research in Science, Engineering and Technology (IJMRSET)

(A Monthly, Peer Reviewed, Refereed, Scholarly Indexed, Open Access Journal)

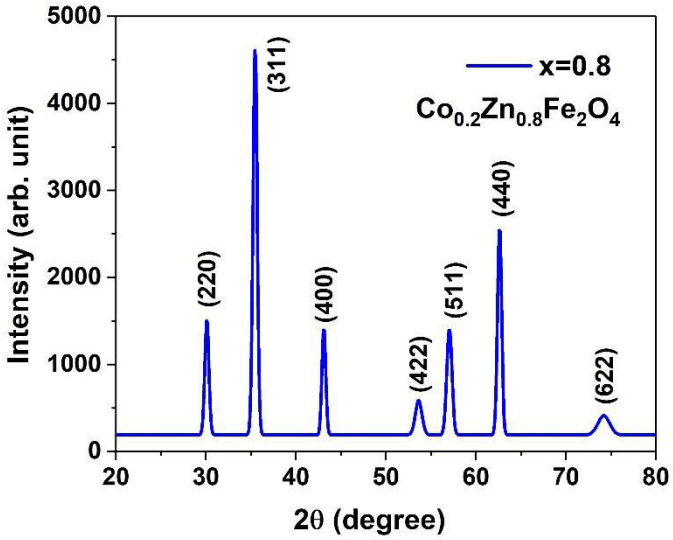

Figure 3. X-ray diffraction pattern of $Co_{1-x}Zn_xFe_2O_4$ (x=0.8) nanoparticles

Table 1. Miller indices of the $Co_{1-x}Zn_xFe_2O_4$ nanoparticles sample x = 0.8

h	k	l	2θ	θ	Sinθ	2Sinθ	d	(a/d)^2	a
2	2	0	30.105	15.053	0.260	0.519	2.965	7.987	8.387
3	1	1	35.466	17.733	0.305	0.609	2.528	10.985	8.386
4	0	0	43.100	21.550	0.367	0.735	2.097	15.976	8.386
4	2	2	53.634	26.817	0.451	0.902	1.707	24.100	8.363
5	1	1	57.049	28.524	0.478	0.955	1.613	27.002	8.380
4	4	0	62.627	31.313	0.520	1.040	1.482	31.983	8.382
6	2	2	74.205	37.102	0.603	1.207	1.277	43.088	8.468
									8.393

Table 1 provides valuable information about the structural properties of $Co_{0.2}Zn_{0.8}Fe_2O_4$ nanoparticles, including details on their crystallographic planes, lattice spacing, and crystal structure. The Miller indices (h, k, l) and diffraction angles (2θ and θ) indicate that the interplanar spacing (d) decreases with increasing diffraction angles, which is typical of a cubic spinel structure. The lattice constant (a) remains consistently around 8.394 Å across different planes, suggesting that the nanoparticles retain a stable cubic lattice. This consistency in the lattice constant confirms the structural integrity of the $Co_{0.2}Zn_{0.8}Fe_2O_4$ nanoparticles [25].

Table 2. FWHM, Crystallite size (D), dislocation density (δ), lattice strain (ε), of $Co_{1-x}Zn_xFe_2O_4$ nanoparticles sample x = 0.8

2θ	θ in Degree	Radian(θ)	FWHM Degree (θ)	FWHM Radian (θ)	Cos θ	D= 0.9λ/βCosθ	D nm	$\delta*10^3$ (nm^{-2})	$\varepsilon*10^{-3}$
30.105	15.052	0.263	0.537	0.009	0.966	153.042	15.304	4.26	0.635
35.466	17.733	0.309	0.546	0.010	0.953	152.591	15.259	4.29	0.763

ISSN: 2582-7219 | www.ijmrset.com | Impact Factor: 7.521| ESTD Year: 2018|

International Journal of Multidisciplinary Research in Science, Engineering and Technology (IJMRSET)

(A Monthly, Peer Reviewed, Refereed, Scholarly Indexed, Open Access Journal)

43.100	21.550	0.376	0.479	0.008	0.930	178.093	17.809	3.15	0.826
53.634	26.817	0.468	0.862	0.015	0.893	103.221	10.322	9.38	1.903
57.049	28.524	0.498	0.662	0.012	0.879	136.549	13.655	5.36	1.571
62.627	31.313	0.546	0.531	0.009	0.854	175.098	17.510	3.26	1.410
74.205	37.102	0.647	1.517	0.026	0.798	65.667	6.567	23.18	5.00
							18.584		

Table 2 offers a comprehensive overview of the structural characteristics of $Co_{1-x}Zn_xFe_2O_4$ nanoparticles with x = 0.8, including Full Width at Half Maximum (FWHM), crystallite size (D), dislocation density (δ), and lattice strain (ε). The data reveal variations in the FWHM values, both in degrees and radians, which indicate the broadening of diffraction peaks. This broadening, in turn, affects the calculated crystallite size, ranging from approximately 65.7 nm to 178.1 nm. The dislocation density, calculated as $\delta = \frac{1}{D^2} \times 10^3$, varies from about 3.15×10^3 nm^{-2} to 23.18×10^3 nm^{-2}, reflecting differences in the quality of the crystal structure across the sample. Similarly, the lattice strain, derived from peak broadening, ranges from 0.635×10^{-3} to 5.00×10^{-3}, highlighting the internal stresses present within the nanoparticles. The relationship between crystallite size, dislocation density, and lattice strain underscores the variability in structural integrity and quality among the nanoparticles, with larger crystallites generally associated with lower dislocation densities and strains, suggesting improved crystallinity [26].

Fourier Infra-red Spectroscopy

The FTIR spectra for $Co_{1-x}Zn_xFe_2O_4$ (x=0.8) nanoparticles, with x = 0.8, as shown in **Figure 4**, reveal several key absorption peaks that provide critical insights into the material's structural and chemical properties. These peaks confirm the formation of spinel ferrite structures and detail the interactions between metal cations and oxygen within the crystal lattice. The first notable absorption band (ν_1) appears around 541 cm^{-1}, indicative of stretching vibrations of metal-oxygen (M-O) bonds at tetrahedral sites [27]. This band is characteristic of the higher-energy vibrations associated with cations like Co^{2+} or Fe^{3+} situated at tetrahedral coordination sites. The position and intensity of this peak suggest a stable tetrahedral coordination, despite the partial substitution of Zn^{2+}. The second absorption band (ν_2) occurs at approximately 409 cm^{-1}, corresponding to metal-oxygen stretching vibrations at octahedral sites. The lower frequency of this band is attributed to the larger size and weaker bonds of the octahedral cations, such as Zn^{2+}, Fe^{3+}, or Co^{2+}. The shift in absorption bands, particularly with the introduction of Zn^{2+}, signifies successful Zn incorporation into the lattice, which alters the local bonding environment and vibrational frequencies [28]. Changes in the intensity and position of these bands reflect distortions in the crystal structure due to substitution. These FTIR findings are crucial as they confirm the structural integrity of the spinel ferrite and shed light on the material's chemical composition and bonding. The incorporation of Zn into the $CoFe_2O_4$ lattice influences the material's physical and magnetic properties, enhancing its suitability for various applications, including catalysis, magnetic data storage, and biomedical technologies. Understanding these vibrational properties and the impact of Zn substitution allows for optimization of the synthesis process and improved performance of these ferrite nanoparticles in technological applications [29].

© 2024 IJMRSET | Volume 7, Issue 9, September 2024| DOI: 10.15680/IJMRSET.2024.0709011

ISSN: 2582-7219 | www.ijmrset.com | Impact Factor: 7.521| ESTD Year: 2018|

International Journal of Multidisciplinary Research in Science, Engineering and Technology (IJMRSET)

(A Monthly, Peer Reviewed, Refereed, Scholarly Indexed, Open Access Journal)

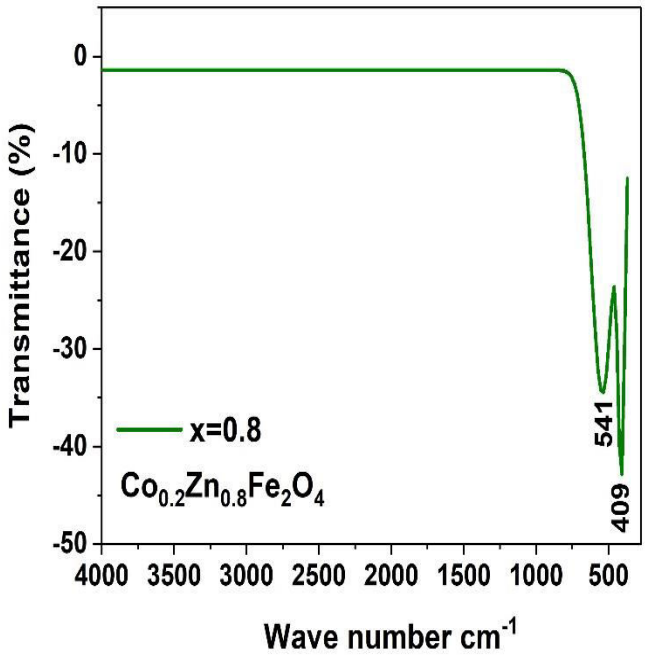

Figure 4 FTIR spectra of $Co_{1-x}Zn_xFe_2O_4$ (x=0.8) nanoparticles

DC- Electrical resistivity

The graph depicting DC resistivity for $Co_{1-x}Zn_xFe_2O_4$ nanoparticles with a composition of (x = 0.8) offers significant insights into the electrical characteristics of the material. In **Figure 5**, the natural logarithm of electrical conductivity (log σ) is plotted against the reciprocal of temperature (1000/T in Kelvin), revealing a distinct dependence on temperature. As the temperature rises (moving from right to left along the x-axis), there is an increase in electrical conductivity, which signifies a reduction in resistivity. This observed relationship adheres to an Arrhenius-type behavior, where conductivity exhibits an exponential increase with temperature. The slope of this graph can be utilized to determine the activation energy (Ea) for conduction, in accordance with the Arrhenius equation [30] $\sigma = \sigma_0 \exp(\frac{E_a}{kT})$ This behavior indicates that the conduction within the material is thermally activated, a hallmark of semiconductors, where charge carriers acquire adequate thermal energy to surpass the activation energy threshold. The particular composition of $Co_{0.2}Zn_{0.8}Fe_2O_4$ suggests that the substitution of Zn^{2+} is crucial to the conduction mechanism. Zn ions, possessing a distinct electronic configuration in comparison to Co^{2+} ions, modify the electronic structure and influence the activation energy required for conduction. This substitution impacts various factors, including the density of states, charge carrier mobility, and the crystal structure, ultimately affecting the overall conductivity. The DC resistivity graph corroborates that $Co_{0.2}Zn_{0.8}Fe_2O_4$ demonstrates thermally activated semiconducting behavior, with conductivity rising alongside temperature, thereby underscoring the influence of Zn^{2+} substitution on the electrical characteristics of the material. [31].

© 2024 IJMRSET | Volume 7, Issue 9, September 2024| DOI: 10.15680/IJMRSET.2024.0709011

ISSN: 2582-7219 | www.ijmrset.com | Impact Factor: 7.521| ESTD Year: 2018|

International Journal of Multidisciplinary Research in Science, Engineering and Technology (IJMRSET)

(A Monthly, Peer Reviewed, Refereed, Scholarly Indexed, Open Access Journal)

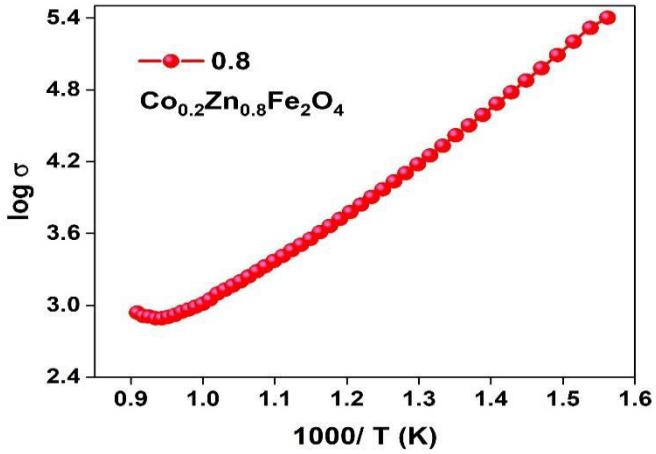

Figure 5 DC-resistivity of $Co_{1-x}Zn_xFe_2O_4$ (x=0.8) nanoparticles

Magnetic property (M-H)

The M-H plot for $Co_{0.2}Zn_{0.8}Fe_2O_4$ nanoparticles with a composition of (x = 0.8) provides important insights into the magnetic properties of the material. The plot shows a typical S-shaped hysteresis loop, characteristic of ferromagnetic materials, indicating strong magnetic interactions. In **Figure 6**, the saturation magnetization (Ms) is approximately 0.65 emu, representing the maximum magnetization achieved when all magnetic moments are aligned with the applied magnetic field. The coercivity (Hc), or the field strength needed to reduce the magnetization to zero after saturation, is indicated by the points where the curve crosses the x-axis [32]. The remanent magnetization (Mr), which is the residual magnetization when the applied field is reduced to zero, is around 0.32 emu. The significant coercivity and remanence confirm the ferromagnetic behavior of $Co_{0.2}Zn_{0.8}Fe_2O_4$ at room temperature. The shape and size of the hysteresis loop indicate strong magnetic interactions typical of spinel ferrites. The substitution of Zn^{2+} has a noticeable influence on the magnetic properties, as it affects the distribution of cations between the tetrahedral and octahedral sites in the spinel structure. This change in cation distribution impacts the overall magnetic behavior, confirming that $Co_{0.2}Zn_{0.8}Fe_2O_4$ is a ferromagnetic material with unique magnetic properties due to the incorporation of Zn^{2+} [33, 34].

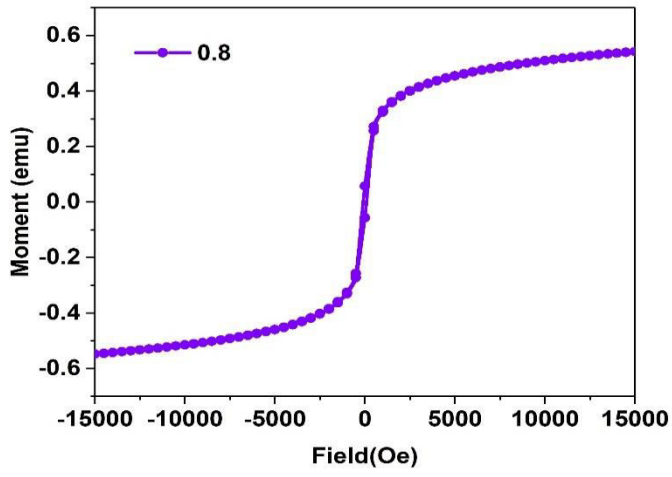

Figure 6 Hysteresis loop of $Co_{1-x}Zn_xFe_2O_4$ (x=0.8) nanoparticles

ISSN: 2582-7219 | www.ijmrset.com | Impact Factor: 7.521| ESTD Year: 2018|

International Journal of Multidisciplinary Research in Science, Engineering and Technology (IJMRSET)

(A Monthly, Peer Reviewed, Refereed, Scholarly Indexed, Open Access Journal)

V. CONCLUSION

The investigation into the structural and morphological characteristics of $Co_{1-x}Zn_xFe_2O_4$ (x = 0.8) nanoparticles, produced through a wet chemical synthesis method, has yielded significant insights regarding the material's attributes. X-ray diffraction analysis confirmed the establishment of a single-phase cubic spinel structure, accompanied by a consistent lattice constant. Fourier-transform infrared spectroscopy (FTIR) revealed distinct vibrations associated with metal-oxygen bonds, thereby validating the spinel ferrite configuration. Calculations derived from XRD data indicated the crystallite size, dislocation density, and lattice strain, which suggest moderate structural imperfections that could affect the magnetic properties of the nanoparticles. Further magnetic assessments exhibited ferromagnetic behavior, characterized by considerable saturation magnetization, coercivity, and remanent magnetization. The incorporation of Zn^{2+} into the $CoFe_2O_4$ lattice resulted in significant alterations to the magnetic properties, offering a pathway to customize the material for specific applications. These $Co_{1-x}Zn_xFe_2O_4$ nanoparticles demonstrate considerable promise for utilization in a range of advanced technologies, such as magnetic devices, sensors, and biomedical applications, owing to their adjustable structural, magnetic, and electrical properties..

REFERENCES

[1] T. Zeeshan, S. Waseem, Z. Ejaz, Z. Kayani, T.E. Kuntsevich, Study of electrical conductance and dielectric properties of vanadium doped cobalt ferrites for high frequency applications, Inorganic Chemistry Communications, 162 (2024) 111687.

[2] B.S. Rao, C.S. Beera, B. Dhanalakshmi, B. Nagarjun, G.N. Raju, Influence of synthesis methods on the structural, dielectric and magnetic properties of Cobalt ferrites, Journal of the Indian Chemical Society, DOI (2024) 101308.

[3] A. Milutinović, Z.Ž. Lazarević, M. Šuljagić, L. Andjelković, Synthesis-Dependent Structural and Magnetic Properties of Monodomain Cobalt Ferrite Nanoparticles, Metals, 14 (2024) 833.

[4] M. Khelfallah, C. Carvallo, V. Dupuis, S. Neveu, D. Taverna, Y. Guyodo, J.-M. Guigner, E. Bertuit, L. Michot, W. Baaziz, Structural and Magnetic Properties of Ferrofluids Composed of Self-Assembled Cobalt Ferrite Nanoflowers: A Multiscale Investigation, The Journal of Physical Chemistry C, 128 (2024) 13162-13176.

[5] A.A. Kajani, A. Pouresmaeili, M. Kamali, Facile one-pot synthesis of the mesoporous chitosan-coated cobalt ferrite nanozyme as an antibacterial and MRI contrast agent, RSC advances, 14 (2024) 16801-16808.

[6] S. Mohana, S. Sumathi, Agaricus bisporus mediated synthesis of cobalt ferrite, copper ferrite and zinc ferrite nanoparticles for hyperthermia treatment and drug delivery, Journal of Cluster Science, 35 (2024) 129-142.

[7] M.A. Hossain, N.Y. Tanisa, R. Awal, M. Ifat-Al-Karim, M.M. Islam, M.M. Haque, M.M. Rahman, Exploration and examination of the structural, optical, thermal, and functional attributes of a hydroxyapatite and cobalt ferrite nanocomposite for biomedical utilization, AIP Advances, 14 (2024).

[8] N. Oroskhani, S.M. Amini, S. Shirvalilou, M. Khodaie, S.R. Mahdavi, Anti‐Proliferative Activity of Poloxamer Cobalt Ferrite Nanoparticles against Human Prostate Cancer (DU‐145) Cells: In‐Vitro Study, IET Nanobiotechnology, 2024 (2024) 8929168.

[9] D. Vinnik, D. Sherstyuk, V. Zhivulin, S. Gudkova, D. Pankratov, N. Perov, Y.A. Alekhina, E. Shipkova, S. Trukhanov, K. Astapovich, Impact of the Zn/Ni concentration on crystal structure and magnetic properties of the Co0. 3Zn0. 7-xNixFe2O4 (0≤ x≤ 0.7) spinel ferrites, Journal of Magnetism and Magnetic Materials, 605 (2024) 172344.

[10] M.A. Darwish, M.M. Hussein, M.K. Omar, W. Abd-Elaziem, Y. Yao, D.S. Klygach, M. Silibin, S.V. Trukhanov, N.V. Abmiotka, D.I. Tishkevich, Crystal structure and peculiarities of microwave parameters of Mg1-xZnxFe2O4 nanospinel ferrites, Ceramics International, 50 (2024) 21027-21039.

[11] R. Arras, K. Sharma, L. Calmels, Interplay between oxygen vacancies and cation ordering in the NiFe 2 O 4 spinel ferrite, Journal of Materials Chemistry C, 12 (2024) 556-561.

[12] S. Gautam, R. Charak, S. Garg, N. Goyal, S. Chakraverty, K.H. Chae, Y. Kim, Probing temperature-dependent magnetism in cobalt and zinc ferrites: A study through bulk and atomic-level magnetic measurements for spintronics, Journal of Magnetism and Magnetic Materials, 593 (2024) 171867.

[13] R. Jasrotia, J. Prakash, Y.B. Saddeek, A.H. Alluhayb, A.M. Younis, N. Lakshmaiya, C. Prakash, K. Aly, M. Sillanpää, Y.A. Ismail, Cobalt ferrites: Structural insights with potential applications in magnetics, dielectrics, and Catalysis, Coordination Chemistry Reviews, 522 (2025) 216198.

ISSN: 2582-7219 | www.ijmrset.com | Impact Factor: 7.521| ESTD Year: 2018|

International Journal of Multidisciplinary Research in Science, Engineering and Technology (IJMRSET)

(A Monthly, Peer Reviewed, Refereed, Scholarly Indexed, Open Access Journal)

[14] S. Mansour, N. Al-Bassami, M. Abdo, Effects of Ce3+ doping on magnetic and dielectric properties of cobalt zinc manganese ferrites for high frequency applications, Ceramics International, 50 (2024) 6165-6174.
[15] M. Hussain, A. Mehmood, F. Ali, Z.A. Sandhu, M.A. Raza, S. Sajid, M. Sohaib, M.T. Khan, A.H. Bhalli, A. Hussain, Tuning the Magnetic Behavior of Zinc Ferrite via Cobalt Substitution: A Structural Analysis, ACS omega, 9 (2024) 2536-2546.
[16] S. Nasrin, F.-U.-Z. Chowdhury, M.M. Hossen, A. Islam, A. Kumar, S.M. Hoque, Investigation of the suitability of zinc-doped cobalt ferrite as hyperthermia heating and MRA contrast agent, Journal of Materials Research, 39 (2024) 501-520.
[17] O. Cadar, T. Dippong, M. Senila, E.-A. Levei, Progress, Challenges and opportunities in divalent transition metal-doped cobalt ferrites nanoparticles applications, Advanced Functional Materials, DOI (2020) 1-17.
[18] K. Sathiyamurthy, C. Rajeevgandhi, L. Guganathan, S. Bharanidharan, S. Savithiri, Enhancement of magnetic, supercapacitor applications and theoretical approach on cobalt-doped zinc ferrite nanocomposites, Journal of Materials Science: Materials in Electronics, 32 (2021) 11593-11606.
[19] H. Mahajan, S.K. Godara, A. Srivastava, Synthesis and investigation of structural, morphological, and magnetic properties of the manganese doped cobalt-zinc spinel ferrite, Journal of Alloys and Compounds, 896 (2022) 162966.
[20] P.A. Vinosha, A. Manikandan, A.S.J. Ceicilia, A. Dinesh, G.F. Nirmala, A.C. Preetha, Y. Slimani, M.A. Almessiere, A. Baykal, B. Xavier, Review on recent advances of zinc substituted cobalt ferrite nanoparticles: Synthesis characterization and diverse applications, Ceramics International, 47 (2021) 10512-10535.
[21] D. Bokov, A. Turki Jalil, S. Chupradit, W. Suksatan, M. Javed Ansari, I.H. Shewael, G.H. Valiev, E. Kianfar, Nanomaterial by sol-gel method: synthesis and application, Advances in materials science and engineering, 2021 (2021) 5102014.
[22] M. Parashar, V.K. Shukla, R. Singh, Metal oxides nanoparticles via sol–gel method: a review on synthesis, characterization and applications, Journal of Materials Science: Materials in Electronics, 31 (2020) 3729-3749.
[23] P.A. Vinosha, A. Manikandan, R. Ragu, A. Dinesh, K. Thanrasu, Y. Slimani, A. Baykal, B. Xavier, Impact of nickel substitution on structure, magneto-optical, electrical and acoustical properties of cobalt ferrite nanoparticles, Journal of Alloys and Compounds, 857 (2021) 157517.
[24] A. Messaoudi, A. Omri, A. Benali, M. Ghebouli, A. Djemli, M. Fatmi, A. Habila, A.A. Alothman, N. Hamdaoui, R. Ajjel, Prediction study of structural, thermal, and optical characterization of Co0. 6Zn0. 4Fe2O4 cubic spinel synthesized via sol–gel method for energy storage, Journal of the Korean Physical Society, DOI (2024) 1-11.
[25] A.A. Ansari, M. Abushad, M. Arshad, S. Naseem, H. Ahmed, S. Husain, W. Khan, Microstructure, optical and dielectric properties of cobalt-doped zinc ferrite nanostructures, Journal of Materials Science: Materials in Electronics, 32 (2021) 21988-22002.
[26] J.P.K. Chintala, S. Bharadwaj, M.C. Varma, G. Choudary, Impact of cobalt substitution on cation distribution and elastic properties of Ni–Zn ferrite investigated by X-ray diffraction, infrared spectroscopy, and Mössbauer spectral analysis, Journal of Physics and Chemistry of Solids, 160 (2022) 110298.
[27] M. Sajjad, K. Ali, Y. Javed, A. Sattar, L. Akbar, A. Nawaz, M.Z. Rashid, K. Rasool, M. Alzaid, Detailed analysis of structural and optical properties of spinel cobalt doped magnesium zinc ferrites under different substitutions, Journal of Materials Science: Materials in Electronics, 31 (2020) 21779-21791.
[28] T. Tatarchuk, A. Shyichuk, Z. Sojka, J. Gryboś, M. Naushad, V. Kotsyubynsky, M. Kowalska, S. Kwiatkowska-Marks, N. Danyliuk, Green synthesis, structure, cations distribution and bonding characteristics of superparamagnetic cobalt-zinc ferrites nanoparticles for Pb (II) adsorption and magnetic hyperthermia applications, Journal of Molecular Liquids, 328 (2021) 115375.
[29] M. Shakil, U. Inayat, M. Arshad, G. Nabi, N. Khalid, N. Tariq, A. Shah, M. Iqbal, Influence of zinc and cadmium co-doping on optical and magnetic properties of cobalt ferrites, Ceramics International, 46 (2020) 7767-7773.
[30] M. Kamran, M. Anis-ur-Rehman, Resistive switching effect in RE-Doped cobalt ferrite nanoparticles, Ceramics International, 48 (2022) 16912-16922.
[31] T. Pydiraju, K.S. Rao, P.A. Rao, M.C. Varma, A.S. Kumar, K. Rao, Co-Cd nanoferrite for high frequency application with phenomenal rise in DC resistivity, Journal of Magnetism and Magnetic Materials, 524 (2021) 167662.
[32] A. Soufi, H. Hajjaoui, W. Boumya, A. Elmouwahidi, E. Baillón-García, M. Abdennouri, N. Barka, Recent trends in magnetic spinel ferrites and their composites as heterogeneous Fenton-like catalysts: A review, Journal of Environmental Management, 367 (2024) 121971.
[33] D.D. Andhare, S.R. Patade, J.S. Kounsalye, K. Jadhav, Effect of Zn doping on structural, magnetic and optical properties of cobalt ferrite nanoparticles synthesized via. Co-precipitation method, Physica B: Condensed Matter, 583 (2020) 412051.
[34] S. Divya, P. Sivaprakash, S. Raja, S.E. Muthu, I. Kim, N. Renuka, S. Arumugam, T.H. Oh, Impact of Zn doping on the dielectric and magnetic properties of CoFe2O4 nanoparticles, Ceramics International, 48 (2022) 33208-33218.

INTERNATIONAL STANDARD SERIAL NUMBER INDIA

INTERNATIONAL JOURNAL OF MULTIDISCIPLINARY RESEARCH

IN SCIENCE, ENGINEERING AND TECHNOLOGY

| Mobile No: +91-6381907438 | Whatsapp: +91-6381907438 | ijmrset@gmail.com |

www.ijmrset.com